



US Army Corps
of Engineers

DTIC Final COPY

WAVE INFORMATION STUDIES
OF US COASTLINES

WIS REPORT 21

2

HINDCAST HURRICANE SWELL FOR THE COAST
OF SOUTHERN CALIFORNIA

by

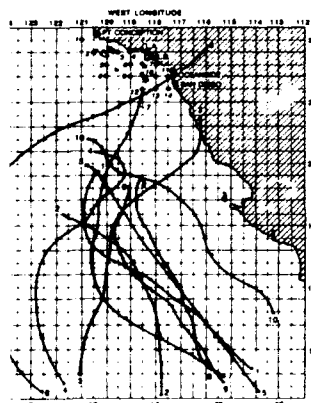
Barbara A. Tracy, Jon M. Hubertz

Coastal Engineering Research Center

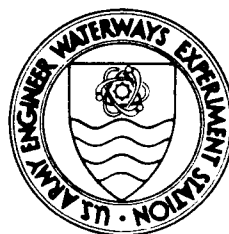
DEPARTMENT OF THE ARMY

Waterways Experiment Station, Corps of Engineers
3909 Halls Ferry Road, Vicksburg, Mississippi 39180-6199

AD-A230 599



DTIC
ELECTE
JAN 11 1991
S B D



November 1990

Final Report

Approved For Public Release; Distribution Unlimited



Prepared for DEPARTMENT OF THE ARMY
US Army Corps of Engineers
Washington, DC 20314-1000

Unclassified

SECURITY CLASSIFICATION OF THIS PAGE

REPORT DOCUMENTATION PAGE				Form Approved OMB No. 0704-0188	
1a. REPORT SECURITY CLASSIFICATION Unclassified			1b. RESTRICTIVE MARKINGS		
2a. SECURITY CLASSIFICATION AUTHORITY			3. DISTRIBUTION/AVAILABILITY OF REPORT Approved for public release; distribution unlimited.		
2b. DECLASSIFICATION/DOWNGRADING SCHEDULE					
4. PERFORMING ORGANIZATION REPORT NUMBER(S) WIS Report 21			5. MONITORING ORGANIZATION REPORT NUMBER(S)		
6a. NAME OF PERFORMING ORGANIZATION USAEWES, Coastal Engineering Research Center		6b. OFFICE SYMBOL (If applicable)	7a. NAME OF MONITORING ORGANIZATION		
6c. ADDRESS (City, State, and ZIP Code) 3909 Halls Ferry Road Vicksburg, MS 39180-6199			7b. ADDRESS (City, State, and ZIP Code)		
8a. NAME OF FUNDING/SPONSORING ORGANIZATION US Army Corps of Engineers		8b. OFFICE SYMBOL (If applicable)	9. PROCUREMENT INSTRUMENT IDENTIFICATION NUMBER		
8c. ADDRESS (City, State, and ZIP Code) Washington, DC 20314-1000			10. SOURCE OF FUNDING NUMBERS		
			PROGRAM ELEMENT NO.	PROJECT NO.	TASK NO.
			WORK UNIT ACCESSION NO.		
11. TITLE (Include Security Classification) Hindcast Hurricane Swell for the Coast of Southern California					
12. PERSONAL AUTHOR(S) Tracy, Barbara A.; Hubertz, Jon M.					
13a. TYPE OF REPORT Final report		13b. TIME COVERED FROM _____ TO _____		14. DATE OF REPORT (Year, Month, Day) November 1990	
15. PAGE COUNT 40					
16. SUPPLEMENTARY NOTATION Available from National Technical Information Service, 5285 Port Royal Road, Springfield, VA 22161.					
17. COSATI CODES			18. SUBJECT TERMS (Continue on reverse if necessary and identify by block number)		
FIELD	GROUP	SUB-GROUP			
19. ABSTRACT (Continue on reverse if necessary and identify by block number)					
<p>This report presents estimates of hurricane-generated swell wave heights and periods at 14 locations along the southern California coastline. Estimates are from a numerical hindcast of winds and waves for 10 hurricanes that occurred between 1956 and 1989. Comparison of hindcast swell height is presented for Hurricane Marie as verification of the hindcast procedure. Mean swell wave height, maximum swell wave height, and maximum period attained during the simulation are presented for each storm at each station. These results characterize the hurricane-generated component of southern swell along the southern California coastline.</p>					
20. DISTRIBUTION/AVAILABILITY OF ABSTRACT <input checked="" type="checkbox"/> UNCLASSIFIED/UNLIMITED <input type="checkbox"/> SAME AS RPT. <input type="checkbox"/> DTIC USERS			21. ABSTRACT SECURITY CLASSIFICATION Unclassified		
22a. NAME OF RESPONSIBLE INDIVIDUAL			22b. TELEPHONE (Include Area Code)		22c. OFFICE SYMBOL

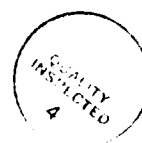
Preface

A project to produce wave climates for US coastal waters began in 1976 at the US Army Engineer Waterways Experiment Station (WES). This project, the Wave Information Study (WIS), was authorized by Headquarters, US Army Corps of Engineers (HQUSACE), as part of the Coastal Field Data Collection Program managed by the WES Coastal Engineering Research Center (CERC). Mr. John H. Lockhart, Jr., was the HQUSACE Technical Monitor.

This report, the 21st in a series, addresses the swell wave component of wave climate along the southern California coast due to hurricanes in the eastern Pacific off the coast of Mexico. The study was conducted at CERC under the direction of Dr. James R. Houston, Chief, CERC; Mr. Charles C. Calhoun, Jr., Assistant Chief, CERC; Mr. H. Lee Butler, Chief, Research Division (RD), CERC; Dr. Edward F. Thompson, former Chief, Coastal Oceanography Branch (COB), RD; and Dr. Martin C. Miller, present Chief, COB. Mr. J. Michael Hemsley was Program Manager for the Coastal Field Data Collection Program. Dr. Jon M. Hubertz was the WIS Project Manager. This report and the data it presents were prepared by Ms. Barbara A. Tracy, COB, and Dr. Hubertz. The authors thank Mmes. Jane B. Payne and Beth Sherard for help with the figures and input data analysis; Ms. Robin D. Reinhard for computer assistance; and Ms. Victoria L. Edwards for word processing, all of the COB.

Commander and Director of WES during report publication was COL Larry B. Fulton, EN. Dr. Robert W. Whalin was Technical Director.

Accession For	
NTIS GRA&I	<input checked="checked" type="checkbox"/>
DTIC TAB	<input type="checkbox"/>
Unannounced	<input type="checkbox"/>
Justification	
By	
Distribution/	
Availability Codes	
Dist	Avail and/or Special
A-1	



Contents

	<u>Page</u>
Preface	1
Introduction	3
Hurricane Selection	5
Hindcasting Procedure	7
Results	10
Verification	11
Conclusion	13
References	15
Bibliography	16
Tables 1-5	
Figures 1-7	
Appendix A: Mean and Maximum Swell Heights and Maximum Periods by Station for Storms 1 Through 10	A1

HINDCAST HURRICANE SWELL FOR THE COAST OF SOUTHERN CALIFORNIA

Introduction

1. This report summarizes swell wave information at 14 stations along the southern California coast produced from a hindcast of 10 hurricanes that occurred between 1956 and 1989 in the eastern Pacific Ocean off the coast of Mexico. Swell produced from hurricanes in this region represents one component of southern swell present along the southern California coast. Southern swell is defined as wave energy generated in distant regions to the south that propagates to the north with little dissipation or change due to local winds. Large storm systems in the south Pacific may also generate swell which may coexist with the hurricane swell component. Lack of directional measurements in deep water makes it difficult to distinguish southern swell from swell generated in the North Pacific. Directional measurements from pressure gage arrays close to shore are of some help, but refraction changes the deepwater direction so that it is difficult to determine the origin of swell. Those directional spectral wave measurements available in the southern California area during hurricane seasons show swell in direction bands that correlate well with tracked hurricane systems. Not many of these measurements are available, however, and data are available only for recent times. Measurements of southern swell as a separate component of the total wave climate are not available.

2. Wave hindcasting can be used to supply southern swell wave information; however, this method is only as accurate as the wind input that drives the wave model. Wind information in the Southern Hemisphere is not as accurate as that available in the Northern Hemisphere due to the relative lack of observations. Thus, at this time, accurate hindcasts of Southern Hemisphere swell are difficult to produce. Hindcasts of southern swell from hurricanes can be done successfully, especially for the more recent storms, when better wind data are available. This study employs the hindcast method to generate hurricane swell information that will add to the qualitative and quantitative description of the wave climate on the southern California coast. This information supplements that provided in Wave Information Study (WIS) Report 20, "Southern California Hindcast Wave Information" (Jensen et al., in preparation). The WIS Report 20 does not include hurricanes because they were not

resolved by the grids used to cover the North Pacific in Phases I and II. The results of these Phase I and II studies were used as boundary conditions for the 20-year southern California study.

3. Two numerical models were used in the hindcast procedure. The first produced wind fields from available hurricane parameters. The second produced wave information using the wind fields as input. This report discusses the hindcasting procedure, summarizes the results, and compares model and measured data. It deals only with the swell waves produced from hurricane systems and does not address those waves generated by local winds along the southern California coastline at the time of the hurricane. The WIS Report 20 (Jensen et al., in preparation) presents the wave climatology along the southern California coastline as derived from a 20-year hindcast using meteorological conditions over the North Pacific Ocean. Results from a similar WIS study on the influence of hurricanes on the Atlantic and Gulf of Mexico coastlines is presented in WIS Report 19 (Abel et al. 1989).

4. Wave hindcasting represents a way to generate data at many evenly spaced locations along the coast at regular time intervals. Measurement devices, which are expensive to purchase, deploy, and maintain, are not available at evenly spaced locations along the coast and, when available, may not be continuous in time over long intervals. This lack of measured data is being addressed by programs both within the US Army Corps of Engineers (COE) and other Federal agencies. A very valuable database of wave measurements exists now and will grow and improve with time. Hindcasting allows more immediate development of a supplementary database covering a long period of time and permits analysis of the information for many locations. Verification of the hindcast procedure using measured data assures the validity of the calculated results.

5. The spectrum of wave energy at a location reflects the total energy in the sea surface from a variety of sources. That portion of the spectrum generated by winds at the site is known as the local wind sea, but there may also be present a component of low-frequency energy generated from a storm system far away from the location. This low-frequency component (swell) travels faster than the local sea due to frequency dispersion as predicted by wave theory and propagates out of its area of generation. The area of generation may be many miles distant from the coastal site of interest. Tropical storms have the potential to produce swell from the large wind waves near their centers. As the storm moves along its path, some of the spectral energy

moves to lower frequencies to create an energy balance in the spectrum. This low-frequency energy continues to radiate from the storm and travels away from the storm with very little dissipation. Since hurricanes represent the strongest type of storms, they have the potential to produce a large amount of swell energy. This swell is evident in wave measurements along the southern California coast during the summer season of the year, which corresponds to the winter season in the Southern Hemisphere.

6. The warm waters off the west coast of Mexico provide a source of energy for tropical storms and hurricanes. These storms typically form from atmospheric waves produced in the equatorial Atlantic Ocean (Simpson and Riehl 1981). The storms that enter the latitudes as far north as southern California usually move along westward paths into the Pacific Ocean. Some of the storms loop eastward and hit the coast of Mexico or the Baja peninsula, but very seldom does a storm move directly into Southern California. Hurricane Hyacinth in 1972 and the hurricane of 1939 are examples of storms that did cross the California coastline. Storm systems that progress northward over cooler water no longer receive energy from a warm ocean surface and usually dissipate to the west.

7. Even though the southern California coast has few direct hurricane hits, it is affected by the addition of low-frequency energy produced from storms passing to the south or west of the area. Directional wave measurements from the National Oceanic and Atmospheric Administration (NOAA) buoy 45024 located at 32.36°N, 117.89°W from May through September 1985 indicate southern swell significant wave heights between 0.5 and 1.5 m. Mean significant swell heights from this hindcast study range from 0.4 to 2.9 m. Maximum significant swell heights from this study range between 0.4 and 4.8 m. During the summer season, this relatively low, but persistent, swell from the south may be the major component of wave climate. Thus, it is important to be able to describe this quantitatively in terms of significant height, peak period, and mean direction for use in engineering studies such as longshore transport estimates and the calculation of wave heights nearshore and within bays and harbors.

Hurricane Selection

8. Sixteen tropical storms are named in an average year in the eastern Pacific; and on the average, eight of these will become hurricanes. This

number of storms represents a typical season for the Pacific coast and corresponds to the summer and fall storm season associated with Atlantic storms. The typhoon season that governs the western Pacific Ocean occurs over a longer period, typically between May and December with the possibility of a storm during any of the other months. Most of the eastern North Pacific storms stay in the area between 10° and 20° N latitude, with only a small percentage advancing north of 24° N latitude.

9. Storms with tracks below 24° N latitude were not included in this study. This decision was based on a test using Hurricane Iselle, August 1984. This storm propagated northward from 17° to 23° N between 110° and 121° W. Maximum wind speeds of 115 knots* were attained at 18.5° N. Hindcast results for this storm indicate that swell generated from this storm did not affect the southern California area. Ten storms fit the above criteria during the period from 1956-1989. The 1956 beginning date corresponds to the beginning date for previous Atlantic, Pacific, and Gulf of Mexico wave information studies, while 1989 was the most recent year for which data were available when the study was done.

10. The paths of these 10 storms crossed above 24° N latitude, and the storms reached hurricane status sometime during their history. Storm information such as dates, track, and storm parameters such as radii, central pressure, and maximum wind speed were obtained from the yearly summary articles presented in the Mariners Weather Log (Mayfield and Gerrish 1988). Less information is available for eastern Pacific hurricanes than for Atlantic storms since they pose less threat to the population and thus are not monitored and sampled as intensely as those in the Atlantic and Gulf of Mexico. The 10 selected storms are listed in Table 1 with the hindcast time period. A map of the eastern North Pacific area with the superimposed tracks is shown in Figure 1. The grid used in Figure 1 has 0.5° latitude and longitude spacing. It extends from 20° to 35° N and from 112° to 125° W. The locations of 14 coastal stations where wave data were saved are also shown.

* To convert knots (international) into metres per second, multiply by 0.5144444.

Hindcasting Procedure

11. Storm track data every 6 hr obtained on magnetic tape from the National Climatic Data Center (NCDC) in Asheville, NC, along with the NOAA Technical Memoranda accompanying them were used to determine the track and central pressure values for the storms. Tracks were linearly interpolated to 1-hr intervals from the 6-hr information. Forward speed and directional heading of the storm were calculated from the track data. Central pressure information was missing for all of the storms at one time or another during their history, but a maximum wind speed was available for these times. For these cases, the following equation was used to estimate the central pressure using the maximum wind speed:

$$P_o = 1,013.0 - \left(\frac{V_{\max}}{6.3} \right)^2 \quad (1)$$

where

P_o = central pressure

V_{\max} = maximum sustained wind speed

Central pressure (P_o) is in millibars, and maximum sustained wind speed (V_{\max}), (10-min average) is in m/sec (Simpson and Riehl, 1981).

12. The North American surface weather charts, obtained on microfilm from NCDC, provided the data at 6-hr intervals to calculate the other parameters needed for input to the wind hindcasting numerical codes. Measurements were made on the weather charts to determine the distance (r) from the center of the storm to a pressure contour. These pressures, their corresponding radial distances, and the central pressure value, P_o , were analyzed by a computer program using the following equation to determine a value of r_a :

$$r_a = r \ln \left(\frac{\Delta P}{P - P_o} \right) \quad (2)$$

where

r_a = scaling factor

ΔP = pressure drop

P = pressure

This r_a value is a scaling factor, described in an unpublished report available from the WIS project office.* It is required by the planetary boundary layer wind model and is not necessarily the radius of maximum winds for the hurricane. The pressure drop ΔP was calculated from $\Delta P = P_\infty - P_0$, where P_∞ is the far field pressure, which is defined as the pressure at that point distant from the center of the storm where the pressure contours no longer have a curvature associated with the storm. The pressure distribution in all the storms hindcast was considered to be radially symmetric.

13. A more extensive discussion of the wind hindcasting procedure for hurricanes is included in WIS Report 19 on Atlantic and Gulf of Mexico hurricanes (Abel et al. 1989). The wind hindcasting procedure produces wind speed and direction at an anemometer height of 10 m, based on the physical representation of the planetary boundary layer of a tropical cyclone. The wind fields, output every hour, represent time averaged winds and do not include gusts. The wind model has been verified using US east coast and Gulf of Mexico storms (see WIS Report 19). Eastern Pacific storms have the same structure and characteristics as Atlantic storms, so the physics embodied in the wind model will produce valid wind fields using the meteorological data available. As an example, Mayfield and Gerrish (1988) report:

The remnants of three Atlantic tropical cyclones became tropical cyclones in the Eastern North Pacific basin. Tropical depression 6 in the Atlantic became Hurricane Kristy in the Eastern North Pacific. Hurricane Debby in the Atlantic became tropical depression 17-E in the Eastern North Pacific. Hurricane Joan in the Atlantic became tropical storm Miriam in the Eastern North Pacific.

14. The wind hindcasting procedure begins by defining a set of snapshots of storm conditions at various times during the storm. The parameters, central pressure, radius, heading, steering velocity, storm forward speed, far field pressure, and the latitude of the center, are defined. Track

* V. J. Cardone, C. V. Greenwood, and J. A. Greenwood, 1979 (Oct), "A Unified Program for the Specification of Hurricane Boundary Layer Winds Over Surfaces of Specified Roughness," unpublished contractor report, US Army Engineer Waterways Experiment Station, Coastal Engineering Research Center, Vicksburg, MS.

information and calculations from the weather chart measurements are compiled for each of the storms to help identify the different phases of the storm. Each of these storm phases corresponds to a certain central pressure, maximum wind velocity, and storm location. This constitutes a snapshot of the actual storm at a time when these parameters are fairly constant. A wind field is constructed numerically using the planetary boundary layer wind model as described in WIS Report 19. Near the center of the storm where the pressure isobars are closer together, more definition is needed, so three different grid spacings are used within the model with the finest spacing of 5 km at the center of the storm and coarser spacings, which are multiples of this, at the outer limits of the storm. When these calculations are completed, wind fields are available for each of the snapshots and represent each different phase of the storm. Next, these conditions are related to location. The storm track is defined so that hourly wind fields on a latitude-longitude grid can be produced. A second computer program takes the hourly track history and the set of wind field snapshots and calculates hourly wind fields on a latitude-longitude grid. Input parameters are available to rotate snapshots or blend two consecutive snapshots so that the storm can change gradually from one snapshot to another. The final wind fields contain only the hurricane conditions. Any winds far from the hurricane center represent background winds from the hurricane system. Background winds from the meteorological systems in which the hurricane is imbedded or other storm systems are not included in the calculated hurricane wind fields.

15. To begin a wave hindcast, a grid of land and water points must be defined. The land water grid for this study is shown in Figure 1. Since the grid intersections are 0.5° apart, not all the small islands could be resolved. The larger islands close to the southern California coast were represented as land points at I,J intersections (11,29), (14,27), and (14,28). Depths at most of the grid points represent deep water as defined by linear wave theory. Some points near the southern California coast represent intermediate and shallow water for the incident waves.

16. The WIS shallow-water wave model was used to compute the wave conditions. A detailed technical description of the model is available from the

WIS project office in two unpublished reports.* This model was recently used to produce 20-years of wave conditions in the southern California area from Point Conception to the Mexican border and is discussed in WIS Report 20 (Jensen et al., in preparation). It was also used to calculate wave information for the Atlantic and Gulf of Mexico hurricanes (see WIS Report 19 (Abel et al. 1989)) and 20 years of nonhurricane wave information in the Gulf of Mexico (see WIS Report 18 (Hubertz and Brooks 1989)). Verification of the model for hurricanes is presented in WIS Report 19.

17. The WIS shallow-water wave model is a two-dimensional (frequency and direction) discrete spectral model that generates and propagates wave energy over an arbitrary depth field. Energy is input from the atmosphere via the wind. Parameterized nonlinear interactions distribute wave energy in the spectrum so that growth of wave energy with time and fetch and its limitation with frequency correspond to empirical data sets. The effects of refraction, shoaling, and depth limitation of wave height are represented in the model. Output can consist of the two-dimensional energy spectrum, but is usually summarized as significant wave height, peak period, and mean direction for sea and swell as a function of time. Sea and swell are defined respectively on the basis of wave growth in the direction of the wind, or nongrowing, lower frequency energy propagating independently of wind direction. The swell wave information produced by the model for the 10 storms of record at the numbered stations shown in Figure 1 is used to characterize the hurricane swell component of wave climate on the southern California coast.

Results

18. Table 2 lists the latitude and longitude for each of the output stations. The geographical location of an island or coastal area nearby is included for reference at each of the stations. The model output was used to produce the graphical summary of swell wave information in Appendix A and quantitative information in Table 3. At each station listed in Appendix A, the mean significant swell wave height, the maximum significant swell wave height, and the maximum peak period are plotted by storm number. The mean was

* D. T. Resio, 1984 (Oct), "Finite Depth Wave Model" and "User's Manual," unpublished contractor reports, US Army Engineer Waterways Experiment Station, Coastal Engineering Research Center, Vicksburg, MS.

calculated from the values generated during the hindcast period. The maximum values were the largest that occurred during the hindcast period. Table 1 gives the beginning and ending dates covered by each hindcast along with the total number of hours hindcast. The amount of swell energy generated at a station is related to the path and strength of the storm. Hurricanes Hyacinth and Norman represent the larger events because their paths were closer to the coast than the other storms. Another storm that occurred in 1939 had a track which brought it northward between 115° and 120°W longitude until it made landfall south of Point Conception. This storm was hindcast in a separate WIS project. A description of the storm was obtained from Horrer (1950). The calculated maximum significant swell wave height and associated peak period at each station are included in Table 4 as an example of a large event in the hurricane swell wave climate on this coastline.

19. If model results agree with measured data available from recent storms, the historical results should also be valid within the uncertainties of the wind data. As mentioned earlier, it is not possible to isolate and measure southern swell generated from hurricanes off the Mexican coast as a separate entity from all other waves in the ocean. However, some measurements that are available during the same time as a recent storm can be used for comparison if assumptions on the origin of the swell are made.

Verification

20. Two sources of measured wave data off the coast of southern California can be used for comparison to modeled results: NOAA and the COE. The National Oceanographic Data Center provides data from the buoys operated by the National Data Buoy Center (NDBC) off the coastlines of the United States. These data consist of summary information such as significant wave height and peak period and more detailed information such as energy estimates as a function of frequency. A very limited amount of directional wave data is available, and unfortunately none for the periods in this study. The NOAA buoys 46024 and 46025 were operational during 1982-1984 off the coast of southern California. Buoy 46024 is just south of Sta 3 in Figure 1, and 46025 is north of Sta 9. The COE, in cooperation with Scripps Institution of Oceanography, also operates a wave measurement program in this area, called the Coastal Data Information Program (CDIP). Information on the NDBC and CDIP stations are listed in Table 5. Those stations designated with type array consist of

nearshore bottom-mounted pressure gages, from which directional estimates can be made. However, since these gages are close to shore, the directions are those of the refracted waves and cannot be used to indicate the source region of the swell energy.

21. Data are not available to compare with the results of all of the hindcast storms because measurements only began in the early 1980's. The best data available for comparison purposes were for Hurricane Marie. Data were also available for the other two recent storms Ismael and Manuel, but show small swell heights with no increase coincident with passage of the storms and no definite southerly direction. Measured data during Marie were available from the CDIP gages, which indicated an increase in swell energy from the south coincident with passage of the storm. Nondirectional data were also available from NOAA buoy 46025. Data from buoy 46024 were not available at this time. Comparisons were made with the swell portion of the spectrum estimated from the measurements since the hindcast did not represent local wind conditions. Energy at periods of 8 sec and longer was considered to be swell energy. A swell significant wave height was calculated from the energy in these period bands. Comparisons to data from CDIP gages are shown in Figures 2 through 5 for Hurricane Marie. Sta 11 at a depth of 750 m is closest to CDIP gage arrays at Oceanside and San Clemente at depths of 9 and 10 m, respectively. Swell heights as a function of time at these locations are shown in Figure 2. After 1200 hr on 9 September, hindcast and measured swell heights agree within 0.5 m or less, and the model reproduces the peak of 1.2 m quite well at Oceanside. The low model values prior to 1200 hr are due to initial building of the wave field over the ocean, sometimes referred to as model spin-up. The peak swell periods at these locations are shown in Figure 3. Periods from the CDIP gages are reported over a range of 3 sec, for example 10 to 12 sec. The midpoint value of the CDIP range is plotted in this figure and the following figures showing swell peak period. After 1200 hr 9 September, hindcast periods are within ± 1 sec of the measured periods. Sta 5 at a depth of 750 m is closest to a CDIP buoy at a depth of 110 m near Begg Rock. Measured and hindcast swell heights at these locations are shown in Figure 4. The hindcast and measured values agree within 0.5 m or less at these locations after 1200 hr on 9 September. Swell peak periods at these locations are shown in Figure 5 and agree within 1 sec. Comparisons of hindcast results at Sta 9 to data from buoy 46025 are shown in Figures 6 and 7. Sta 9 at a depth of 750 m is closest to buoy 46025 at a depth of 200 m.

Energy at periods of 8 sec and greater was again used to produce a swell wave height from the measured NOAA buoy data. Directional information was not available from the NOAA data, so it is assumed that this swell was from the south. The swell heights hindcast by the model are generally within the accuracy of the buoy up to 1400 hr on 10 September (Figure 6). The accuracy of the NOAA measurements is stated as ± 0.2 m or 5 percent (Gilhousen et al. 1990). The disagreement after this time is probably due to overestimation of wind speeds in the decaying storm. Periods agree within 1 sec after 1600 hr, 9 September. Prior to this time, the buoy is indicating larger periods that may be swell from another source.

22. Several aspects of the hindcasting procedure make comparisons difficult. The hindcast included only the hurricane winds. Local storms or events to the north or west of the area may produce waves that mask the effects of the hurricane. The CDIP spectral information is categorized by frequency bands and may include swell from storms other than hurricanes. Directions of the CDIP data are affected by refraction nearshore. Variation in water depth between the hindcast grid point and the measured station may cause some differences in wave height. The hindcast grid did not represent bathymetric features smaller than 30 nautical miles*; thus the effects of shoal areas and islands are not modeled. Despite these difficulties, the results of the study appear to be well verified, as shown by the comparisons to measurements during Hurricane Marie and previous verifications of the wind and wave model presented in WIS Report 19 (Abel et al. 1989).

Conclusion

23. The 10 storms hindcast in this report are typical of storms reaching this far north. This study indicates the magnitude of significant swell wave height and peak period that could occur in storms with similar tracks. The maximum conditions produced over the period are an indication of the maximum swell conditions that may occur from hurricanes to the south. The time series of significant wave height, peak period, and mean direction at each of the stations is available for each storm. However, since the local wind conditions were not represented, these time series represent only the swell wave

* To convert US nautical miles into kilometres, multiply by 1.852.

field for the storms that passed quite a distance away and do not represent the actual local wave conditions.

24. The information in this report should be used to supplement the wave information in WIS Report 20 (Jensen et al., in preparation), which describes the wave climate in this region exclusive of the southern swell component. Note that the hurricane contribution is only part of the total southern swell component. Swell generated from other storms to the south may be present. A quantitative description of southern swell based on available meteorological information is a difficult problem and needs to be studied further before a hindcast of the complete wave climate in this area is possible. Until that time, it is recommended that studies dependent on wave information use estimates of significant wave height, peak period, and mean direction from the 20-year and hurricane climatology independently, or combine spectra from the two climatologies by linear superposition to obtain a more complete estimate of wave effects.

References

- Abel, C. E., Tracy, B. A., Vincent, C. L., and Jensen, R. E. 1989 (Apr). "Hurricane Hindcast Methodology and Wave Statistics for Atlantic and Gulf Hurricanes from 1956-1975," WIS Report 19, US Army Engineer Waterways Experiment Station, Vicksburg, MS.
- Gilhousen, D. B., Meindl, E. A., Changery, M. J., Franks, P. L., Burgin, M. G., and McKittrick, D. A. 1990 (Feb). "Climatic Summeries for NDBC Data Buoys and Stations Update 1," National Weather Service, National Data Buoy Center, National Science and Technology Laboratory, MS.
- Horrer, P. L. 1950 (Jul). "Southern Hemisphere Swell and Waves from a Tropical Storm at Long Beach, California," Bulletin of the Beach Erosion Board, Vol 4, No. 3.
- Hubertz, J. M., and Brooks, R. M. 1989 (May). "Gulf of Mexico Hindcast Wave Information," WIS Report 18, US Army Engineer Waterways Experiment Station, Vicksburg, MS.
- Jensen, R. E., Hubertz, J. M., Thompson, E. F., Reinhard, R. D., Groves, B. J., Brown, W. A., Payne, J. B., Brooks, R. M., and McAneny, D. S. "Hindcast Wave Information for Southern California," WIS Report 20 in preparation, US Army Engineer Waterways Experiment Station, Vicksburg, MS.
- Mayfield, M., and Gerrish, H. P. 1988 (Summer). "Eastern North Pacific Hurricanes - 1988," Mariners Weather Log.
- Simpson, R. H., and Riehl, H. 1981. The Hurricane and Its Impact, Oxford University Press, Oxford, Great Britain.

Bibliography

- Baum, R. A. 1966 (Mar). "Eastern North Pacific Tropical Cyclones for 1965," Mariners Weather Log, Vol 10, No. 2, pp 38-43.
- _____. 1967 (Mar). "Eastern North Pacific Tropical Cyclones for 1966," Mariners Weather Log, Vol 11, No. 2, pp 47-51.
- _____. 1973 (Apr). "1972 Eastern North Pacific Tropical Cyclones," Monthly Weather Review, Vol 100, pp 343.
- _____. 1975 (Mar). "Eastern North Pacific Tropical Cyclones for 1974," Mariners Weather Log, Vol 19, pp 75-84.
- _____. 1976 (Mar). "Eastern North Pacific Tropical Cyclones for 1975," Mariners Weather Log, Vol 20, pp 125-135.
- Benkman, W. E. 1963 (Mar). "Tropical Cyclones in the Eastern North Pacific for 1962," Mariners Weather Log, Vol 7, No. 2, pp 46-49.
- Crooks, R. C. 1960 (Mar). "Tropical Cyclones in the Eastern North Pacific for 1959," Mariners Weather Log, Vol 4, No. 2, pp 29-32.
- Denney, W. J. 1971 (Mar). "Eastern North Pacific Tropical Cyclones for 1970," Mariners Weather Log, Vol 15, No. 2, pp 67-73.
- _____. 1972 (Mar). "Eastern North Pacific Tropical Cyclones for 1971," Mariners Weather Log, Vol 16, No. 2, pp 76-86.
- Gunther, E. B. 1977 (Mar). "Eastern North Pacific Tropical Cyclones for 1976," Mariners Weather Log, Vol 21, pp 143-154.
- _____. 1978 (Mar). "Eastern North Pacific Tropical Cyclones for 1977," Mariners Weather Log, Vol 22, pp 157-166.
- _____. 1979. "Eastern North Pacific Tropical Cyclones for 1978," Mariners Weather Log, Vol 23, No. 3, pp 152-165.
- _____. 1980. "Eastern North Pacific Tropical Cyclones for 1979," Mariners Weather Log, Vol 24, No. 3, pp 174-182.
- _____. 1981. "Eastern North Pacific Tropical Cyclones for 1980," Mariners Weather Log, Vol 25, No. 3, pp 153-160.
- _____. 1982. "Eastern North Pacific Tropical Cyclones for 1981," Mariners Weather Log, Vol 26, No. 2, pp 59-65.
- _____. 1983. "Eastern North Pacific Tropical Cyclones for 1982," Mariners Weather Log, Vol 27, No. 2, pp 67-76.
- Gunther, E. B., and Cross, R. L. 1984. "Eastern North Pacific Tropical Cyclones for 1983," Mariners Weather Log, Vol 28, No. 2, pp 67-78.
- Gustafson, A. F. 1968 (Mar). "Eastern North Pacific Tropical Cyclones for 1967," Mariners Weather Log, Vol 12, No. 2, pp 42-47.
- _____. 1969 (Mar). "Eastern North Pacific Tropical Cyclones for 1968," Mariners Weather Log, Vol 13, No. 2, pp 48-52.
- _____. 1970 (Mar). "Eastern North Pacific Tropical Cyclones for 1969," Mariners Weather Log, Vol 14, No. 2, pp 62-66.

Jarvinen, B. R., Neumann, C. J., and Davis, M. A. S. 1984 (Mar). "A Tropical Cyclone Data Tape for the North Atlantic Basin, 1886-1983: Contents, Limitations, and Uses," NOAA Technical Memorandum NWS NHC 22, National Hurricane Center, Miami, FL.

Jensen, R. E., Vincent, C. L., and Abel, C. E. 1987 (Jun). "A User's Guide to SHALWV: Numerical Model for Simulation of Shallow-Water Wave Growth, Propagation, and Decay; Report 2, SHALWV-Hurricane Wave Modeling and Verification," Instruction Report CERC-86-2, US Army Engineer Waterways Experiment Station, Vicksburg, MS.

Jensen, R. E., Vincent, C. L., and Reinhard, R. D. 1989 (Apr). "A Multi-Faceted Wind-Wave Hindcast Method to Describe a Southern California Wave Climate," Second International Workshop on Wave Hindcasting and Forecasting.

Mariners Weather Log. 1985. "Eastern North Pacific Tropical Cyclones for 1984," Vol 29, No. 2, p 65.

McGurrian, M. 1965 (Mar). "Tropical Cyclones in the Eastern North Pacific for 1964," Mariners Weather Log, Vol 9, No. 2, pp 42-45.

Monthly Weather Review. 1985 (Aug). "Eastern North Pacific Tropical Cyclones for 1984," Vol 113, pp 1396-1398.

Mull, M. W. 1961 (Mar). "Tropical Cyclones in the Eastern North Pacific for 1960," Mariners Weather Log, Vol 5, No. 2, pp 34-36.

_____. 1962 (Mar). "Tropical Cyclones in the Eastern North Pacific for 1961," Mariners Weather Log, Vol 6, No. 2, pp 44-46.

National Weather Service. 1986 (Apr). Climatic Summaries for NDBC Buoys. National Data Buoy Center, National Science and Technology Laboratory, MS.

Quinn, E. H. 1957 (Mar). "Tropical Storms of the Eastern North Pacific for 1956," Mariners Weather Log, Vol 1, No. 2, pp 25-26.

_____. 1959 (Mar). "Tropical Storms in the Eastern North Pacific for 1958," Mariners Weather Log, Vol 3, No. 2, pp 37-39.

US Army Corps of Engineers. "Monthly Report-August 1983," Coastal Data Information Program, State of California, The Resources Agency, Department of Boating and Waterways, Monthly Summary Report No. 93.

_____. "Monthly Report-September 1983," Coastal Data Information Program. State of California, The Resources Agency, Department of Boating and Waterways, Monthly Summary Report No. 94.

_____. "Monthly Report-September 1984," Coastal Data Information Program, State of California, The Resources Agency, Department of Boating and Waterways, Monthly Summary Report No. 106.

Weaver, S. P., and Kidder, S. Q. 1984. "On the Use of Wind Shear and Vorticity Difference in Forecasting Eastern Pacific Tropical Cyclone Formation," 15th Conference on Hurricanes and Tropical Meteorology, 9-13 January 1984, Miami, FL, American Meteorological Society, pp 276-280.

Wilgus, R. V. 1958 (Mar). "Eastern North Pacific Tropical Storms for 1957," Mariners Weather Log, Vol 2, No. 2, pp 34-37.

_____. 1965 (Mar). "Tropical Cyclones in the Eastern North Pacific for 1963," Mariners Weather Log, Vol 8, No. 2, pp 38-40.

Wilson, E. E. 1974 (Mar). "Eastern North Pacific Tropical Cyclones for 1973," Mariners Weather Log, Vol 18, pp 78-86.

Table 1
Pacific Hurricane List

<u>Storm</u>	<u>Yr/Mo</u>	<u>Name</u>	<u>Beginning Date*</u>	<u>Ending Date*</u>	<u>Hours Simulated</u>
1	5708	no name	57081206	57081512	79
2	6009	Estelle	60090606	60090912	79
3	6309	Katherine	63091612	63091806	43
4	6709	Lily	67090818	67091112	67
5	7208	Gwen	72082806	72083100	67
6	7209	Hyacinth	72090312	72090700	85
7	7808	Norman	78090306	78090600	67
8	8308	Ismael	83081118	83081412	67
9	8309	Manuel	83091712	83091918	55
10	8409	Marie	84090800	84091100	73

* Dates are represented by year, month, day, and hour as YYYYMMDDHH and are in Greenwich Mean Time (GMT).

Table 2
WIS Station Locations

<u>Station</u>	<u>Latitude °N</u>	<u>Longitude °W</u>	<u>Location</u>
1	34.5	121.0	West of Point Conception
2	34.0	120.5	West of Santa Rosa Island
3	34.0	119.5	East of Santa Cruz Island
4	34.0	119.0	Southeast of Point Mugu
5	33.5	120.0	South of Santa Rosa Island
6	33.5	119.0	East of Santa Barbara Island
7	33.5	118.0	South of Huntington Beach
8	33.0	120.0	Southwest of San Nicolas Island
9	33.0	119.0	South of Santa Barbara Island
10	33.0	118.0	East of San Clemente Island
11	33.0	117.5	West of Del Mar
12	32.5	118.5	South of San Clemente Island
13	32.5	118.0	Southeast of San Clemente Island
14	32.5	117.5	West of US-Mexican Border

Table 3
Average and Maximum Swell and Maximum Peak Period

<u>Storm No.</u>	<u>HSAVE, m*</u>	<u>HSMAX, m**</u>	<u>TPMAX, sec†</u>
<u>Station 1</u>			
1	1.5	2.0	12.5
2	1.3	2.1	12.5
3	1.1	1.1	8.3
4	1.5	2.6	12.5
5	1.4	1.7	11.1
6	2.2	2.9	11.1
7	1.8	2.2	12.5
8	0.9	1.4	14.3
9	0.6	0.8	12.5
10	1.1	1.7	10.0
<u>Station 2</u>			
1	1.6	2.2	12.5
2	1.3	2.1	11.1
3	1.2	1.3	9.1
4	1.7	2.9	12.5
5	1.6	2.0	10.0
6	2.3	3.2	11.1
7	2.0	2.7	11.1
8	1.0	1.5	12.5
9	0.8	0.9	12.5
10	1.3	1.8	9.1
<u>Station 3</u>			
1	1.2	2.2	14.3
2	1.2	1.7	11.1
3	1.0	1.2	10.0
4	1.6	2.7	11.1
5	0.9	1.6	12.5
6	2.1	3.0	11.1
7	1.1	2.4	12.5
8	0.9	1.4	14.3
9	0.6	0.8	12.5
10	0.8	1.6	12.5

(Continued)

* HSAVE is the average significant swell wave height that occurred during the simulation.

** HSMAX is the maximum significant swell wave height that occurred during the simulation.

† TPMAX is the maximum peak period that occurred during the simulation.

(Sheet 1 of 4)

Table 3 (Continued)

<u>Storm No.</u>	<u>HSAVE, m</u>	<u>HSMAX, m</u>	<u>TPMAX, sec</u>
<u>Station 4</u>			
1	1.1	1.9	12.5
2	1.0	1.4	12.5
3	0.8	1.1	11.1
4	1.5	2.6	12.5
5	0.8	1.4	12.5
6	2.0	2.9	10.0
7	1.5	2.2	12.5
8	0.8	1.0	12.5
9	0.5	0.6	12.5
10	1.0	1.4	12.5
<u>Station 5</u>			
1	1.7	2.6	12.5
2	1.5	2.1	11.1
3	1.4	1.6	9.1
4	2.0	3.3	12.5
5	1.6	2.1	10.0
6	2.5	3.4	11.1
7	2.2	3.2	11.1
8	1.1	1.6	12.5
9	0.9	1.1	11.1
10	1.2	2.0	10.0
<u>Station 6</u>			
1	1.3	2.3	14.3
2	1.2	1.7	11.1
3	1.1	1.4	11.1
4	1.8	3.0	12.5
5	1.1	1.7	12.5
6	2.2	3.4	10.0
7	1.7	2.5	12.5
8	1.0	1.3	12.5
9	0.7	0.9	12.5
10	1.1	1.6	12.5
<u>Station 7</u>			
1	1.2	1.7	12.5
2	1.2	1.7	12.5
3	0.9	1.0	11.1
4	1.6	2.4	12.5
5	0.4	0.7	10.0
6	2.4	3.2	10.0
7	1.1	3.1	12.5
8	0.6	0.7	10.0
9	0.4	0.4	9.1
10	0.4	1.4	9.1

(Continued)

(Sheet 2 of 4)

Table 3 (Continued)

<u>Storm No.</u>	<u>HSAVE, m</u>	<u>HSMAX, m</u>	<u>TPMAX, sec</u>
<u>Station 8</u>			
1	2.0	2.9	12.5
2	1.6	2.3	11.1
3	1.7	1.9	10.0
4	2.3	3.7	12.5
5	1.6	2.4	10.0
6	2.5	3.7	11.1
7	2.5	3.6	11.1
8	1.2	1.7	12.5
9	1.0	1.2	11.1
10	1.5	2.3	9.1
<u>Station 9</u>			
1	1.7	2.7	12.5
2	1.5	2.0	11.1
3	1.8	2.0	11.1
4	2.4	3.6	12.5
5	1.6	2.2	11.1
6	2.7	4.1	11.1
7	2.7	3.7	11.1
8	1.2	1.7	12.5
9	0.9	1.2	11.1
10	1.7	2.0	11.1
<u>Station 10</u>			
1	1.5	2.2	12.5
2	1.6	2.2	12.5
3	1.7	2.1	11.1
4	2.1	3.2	12.5
5	0.9	1.8	11.1
6	2.9	4.4	11.1
7	1.6	3.9	12.5
8	1.0	1.4	12.5
9	0.8	1.1	10.0
10	1.3	1.6	12.5
<u>Station 11</u>			
1	0.8	1.3	12.5
2	0.9	1.2	9.1
3	0.6	0.6	10.0
4	1.2	2.0	12.5
5	0.4	0.6	10.0
6	2.6	3.9	11.1
7	0.9	3.1	11.1
8	0.7	0.9	11.1
9	0.7	0.9	10.0
10	0.6	1.3	11.1

(Continued)

(Sheet 3 of 4)

Table 3 (Concluded)

<u>Storm No.</u>	<u>HSAVE, m</u>	<u>HSMAX, m</u>	<u>TPMAX, sec</u>
<u>Station 12</u>			
1	1.8	2.7	12.5
2	1.7	2.1	11.1
3	2.0	2.4	11.1
4	2.8	3.9	11.1
5	1.4	2.2	11.1
6	2.8	4.5	11.1
7	2.6	4.0	11.1
8	1.2	1.7	12.5
9	1.1	1.4	10.0
10	1.5	2.0	12.5
<u>Station 13</u>			
1	1.6	2.4	12.5
2	1.7	2.3	12.5
3	2.0	2.4	11.1
4	2.5	3.5	12.5
5	1.0	2.0	12.5
6	2.9	4.8	11.1
7	2.0	4.1	12.5
8	1.1	1.5	12.5
9	1.0	1.3	10.0
10	1.1	1.8	12.5
<u>Station 14</u>			
1	1.3	2.2	12.5
2	1.7	2.4	12.5
3	1.7	2.3	11.1
4	2.1	3.2	12.5
5	1.0	1.8	11.1
6	2.5	4.6	12.5
7	1.3	3.9	11.1
8	1.0	1.2	12.5
9	1.0	1.2	9.1
10	1.2	1.5	12.5

Table 4
Maximum Swell Significant Wave Height and Associated
Peak Period for the Storm of 1939

<u>Station</u>	<u>Height, m</u>	<u>Period, sec</u>
1	4.0	12.5
2	4.5	12.5
3	3.6	12.5
4	3.5	12.5
5	5.0	12.5
6	4.1	12.5
7	4.5	12.5
8	5.9	12.5
9	5.6	12.5
10	5.2	12.5
11	3.9	12.5
12	5.9	14.3
13	4.9	12.5
14	4.3	12.5

Table 5
Gage Locations

<u>Gage Name</u>	<u>Type</u>	<u>Location</u>				<u>Depth m</u>
		<u>N. Lat.*</u>		<u>W. Long.*</u>		
NOAA Buoy 46024	Buoy	33 48.0		119 30.0		1,650
NOAA Buoy 46025	Buoy	33 6.0		119 0.0		200
Del Mar	Array	32 57.4		117 16.7		11
Oceanside Beach	Array	33 11.4		117 23.4		9
San Clemente	Array	33 24.9		117 37.8		10
Begg Rock	Buoy	33 24.2		119 40.1		110
Santa Cruz Is.	Buoy	33 58.3		119 38.5		55

* Degrees, minutes to tenths.

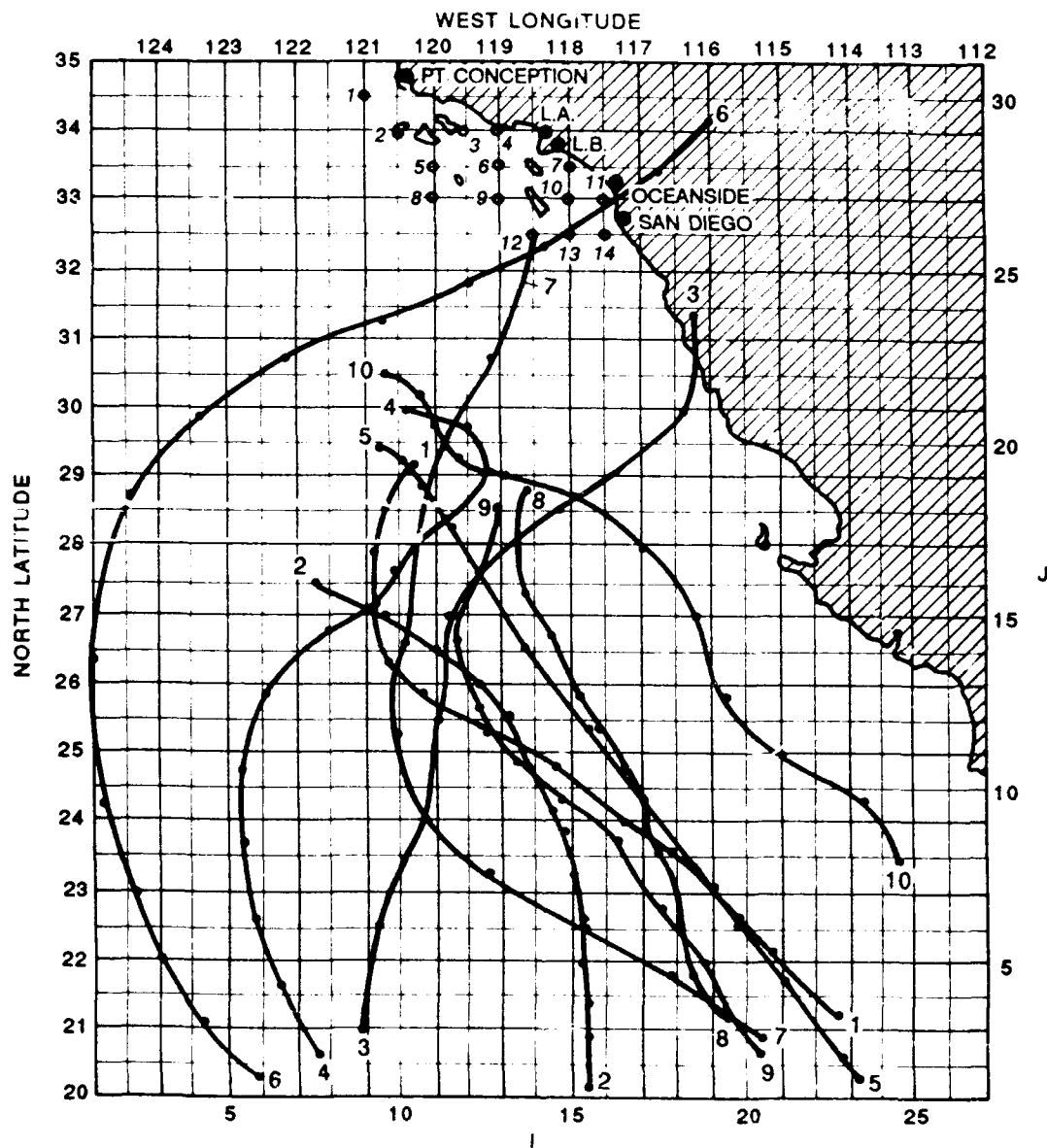


Figure 1. Tracks of hindcast hurricanes (solid numbered lines) and stations (numbered grid intersections) where hindcast results are saved

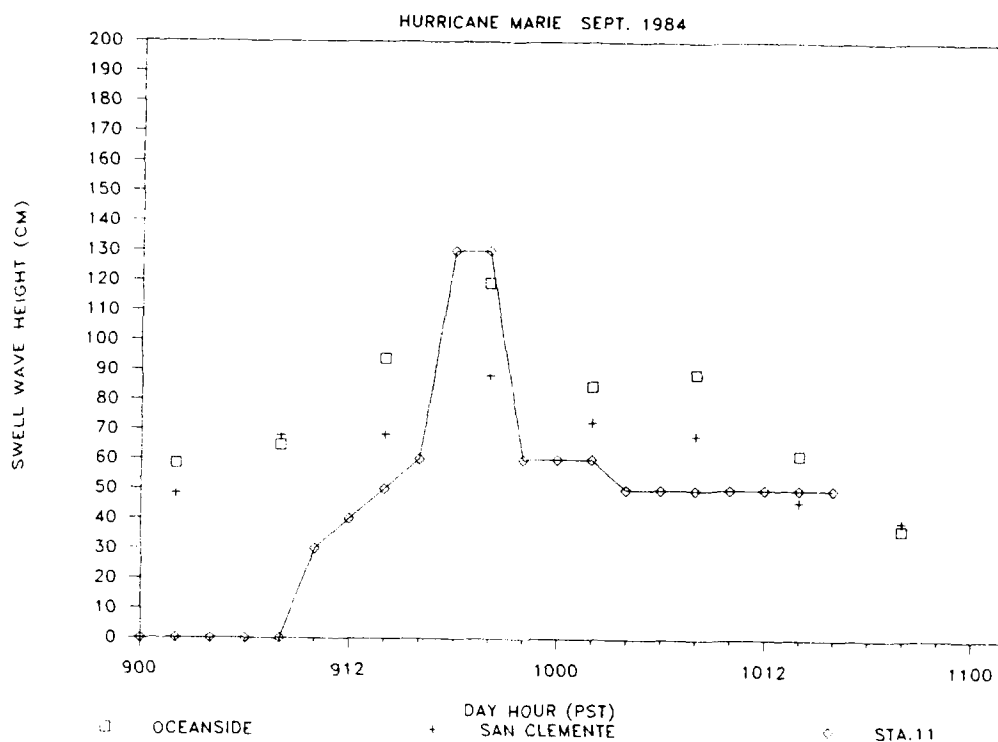


Figure 2. Hindcast swell wave height at Sta 11 and measured swell height at CDIP gage locations Oceanside and San Clemente during Hurricane Marie

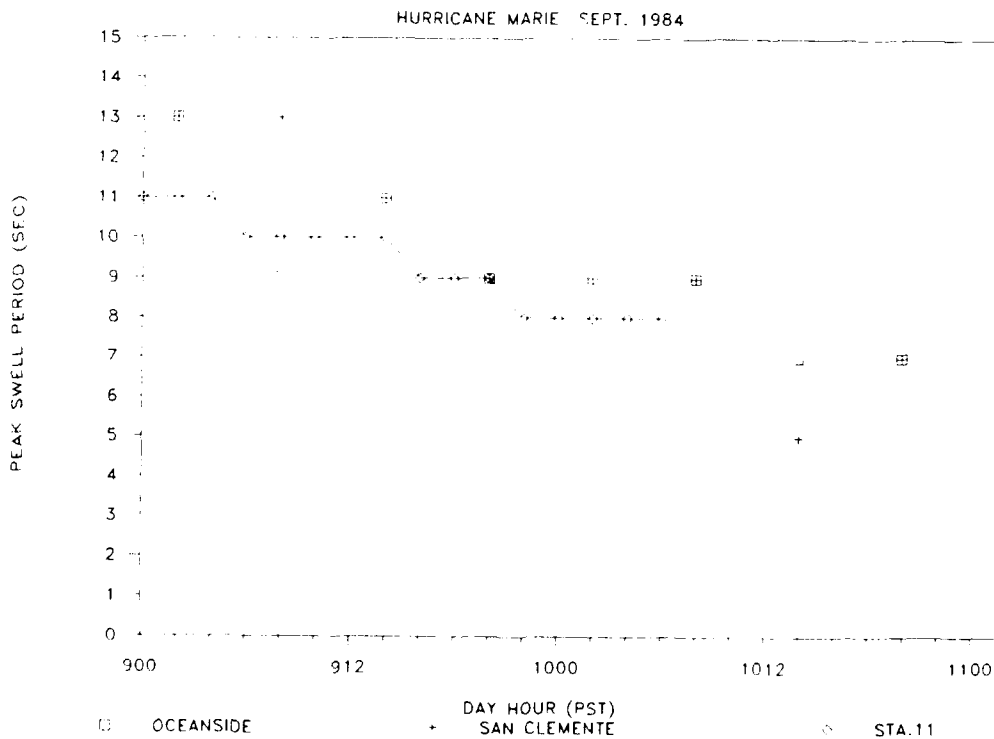


Figure 3. Hindcast swell peak period at Sta 11 and measured swell peak period at CDIP gage locations Oceanside and San Clemente during Hurricane Marie

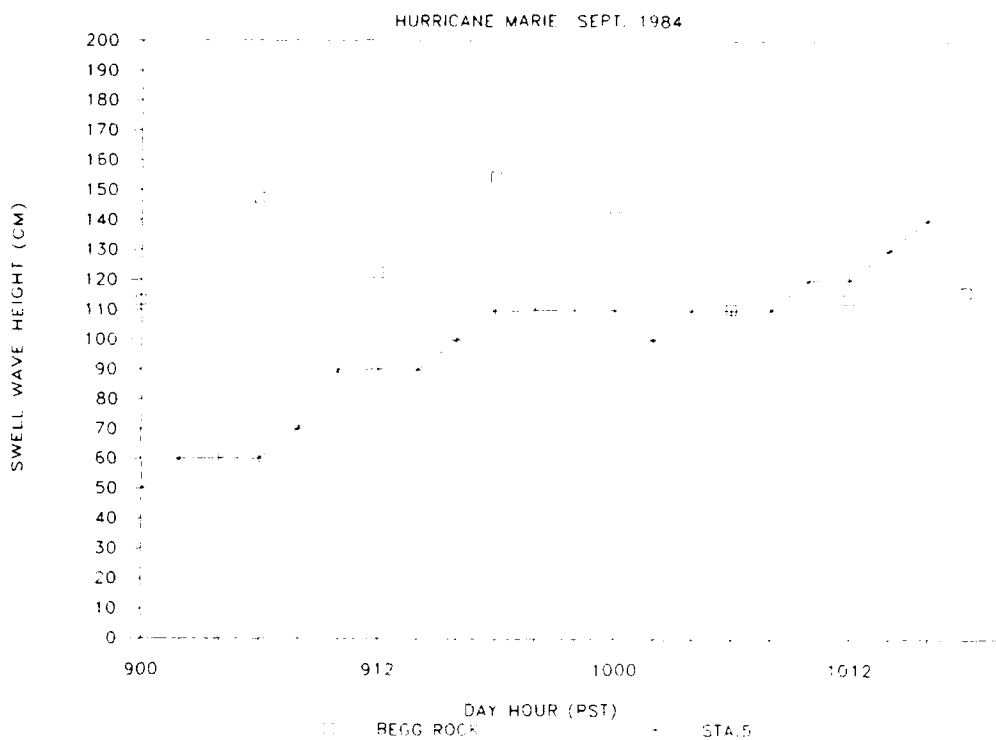


Figure 4. Hindcast swell wave height at Sta 5 and measured swell height at CDIP gage location Begg Rock during Hurricane Marie

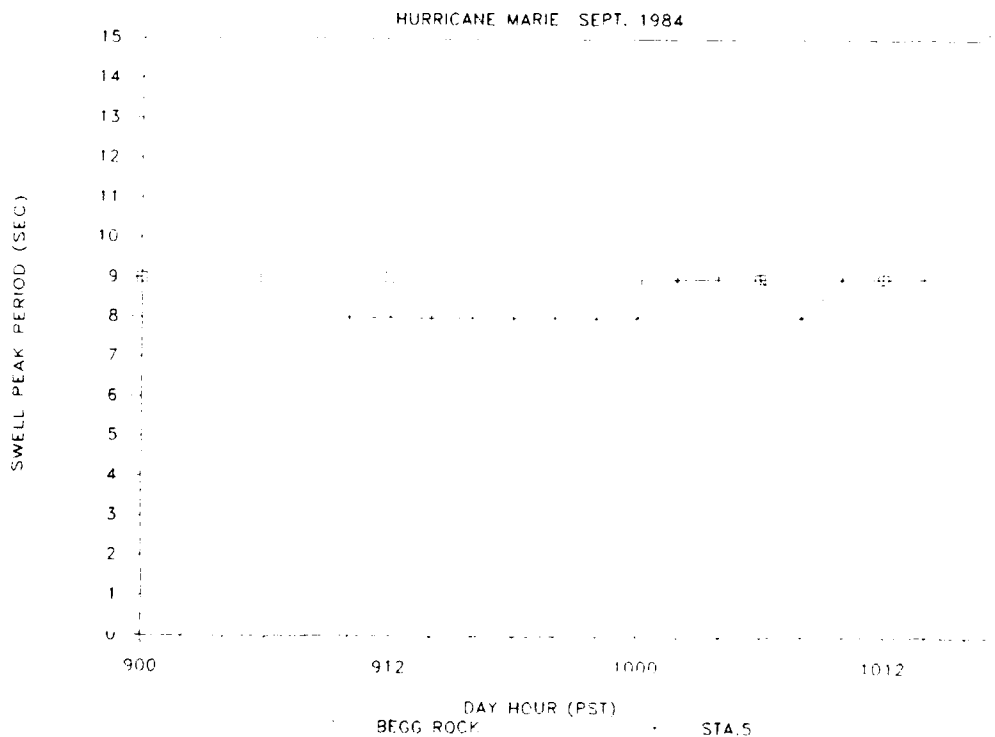


Figure 5. Hindcast swell peak period at Sta 5 and measured swell peak period at CDIP gage location Begg Rock during Hurricane Marie

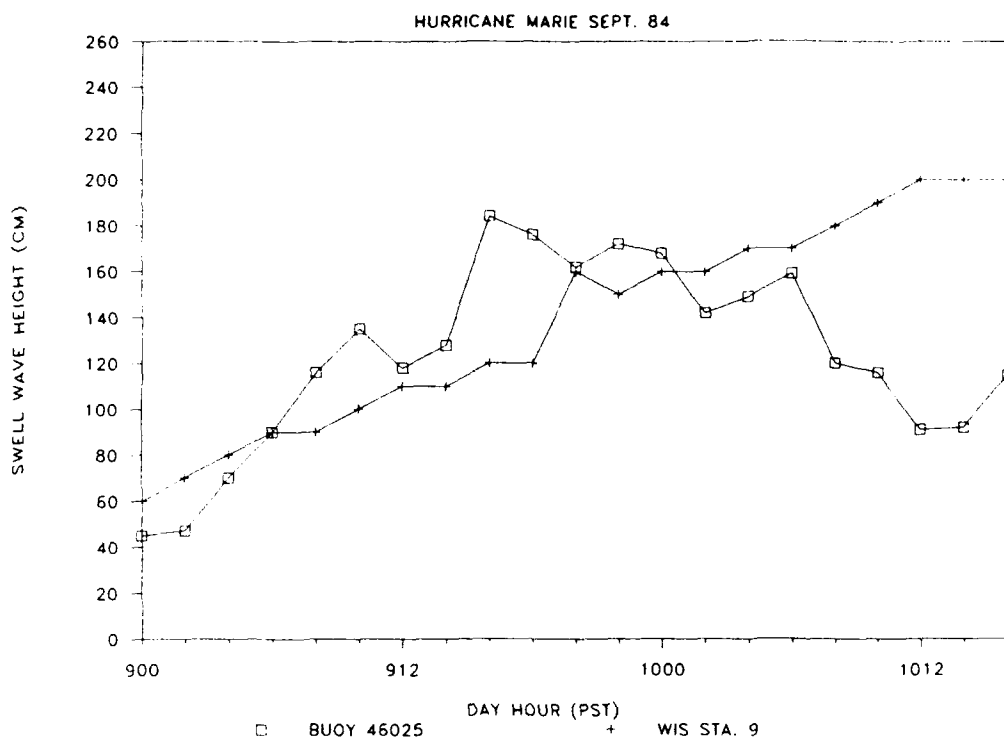


Figure 6. Hindcast swell wave height at Sta 9 and measured swell height at NOAA buoy location 46025 during Hurricane Marie

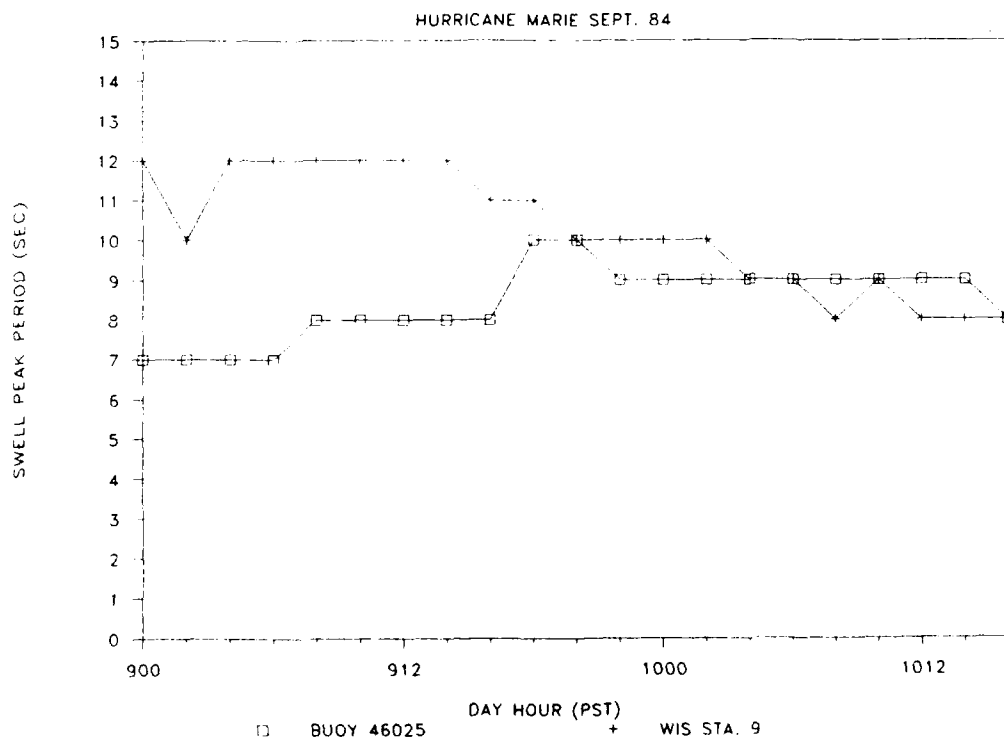


Figure 7. Hindcast swell peak period at Sta 9 and measured swell peak period at NOAA buoy location 46025 during Hurricane Marie

Appendix A: Mean and Maximum Swell Heights and Maximum Periods
by Station for Storms 1 Through 10

